

Supporting Information for

Water Oxidation Catalysis with Nonheme Iron Complexes under Acidic and Basic Conditions: Homogeneous or Heterogeneous?

Dachao Hong,[†] Sukanta Mandal,[‡] Yusuke Yamada,[†] Yong-Min Lee,[‡] Wonwoo Nam,^{*,‡} Antoni Llobet,^{*,§,‡} and Shunichi Fukuzumi^{*,†,‡}

[†] *Department of Material and Life Science, Graduate School of Engineering, ALCA, Japan
Science and Technology Agency, Osaka University, Suita, Osaka 565-0871, Japan*

[‡] *Department of Bioinspired Science, Ewha Womans University, Seoul, 120-750, Korea*

[§] *Institute of Chemical Research of Catalonia (ICIQ), Avinguda Països Catalans 16, E-43007
Tarragona, Spain*

* To whom correspondence should be addressed.

E-mail: fukuzumi@chem.eng.osaka-u.ac.jp, wwnam@ewha.ac.kr, allobet@ICIQ.ES

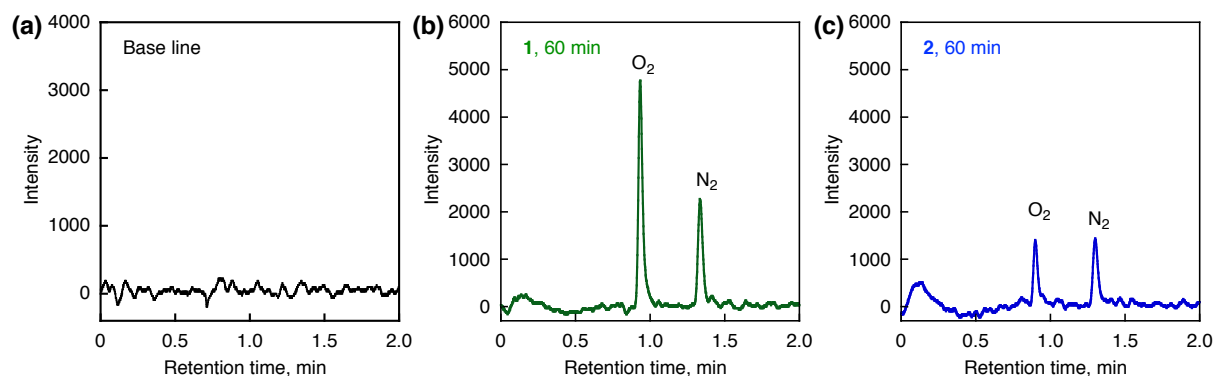


Figure S1. GC charts of (a) a base line and the gas evolved at 60 min in the catalytic water oxidation with (b) **1** (12.5 μ M) and (c) **2** (12.5 μ M) by CAN (125 mM) in a non-buffered aqueous solution (2.0 mL).

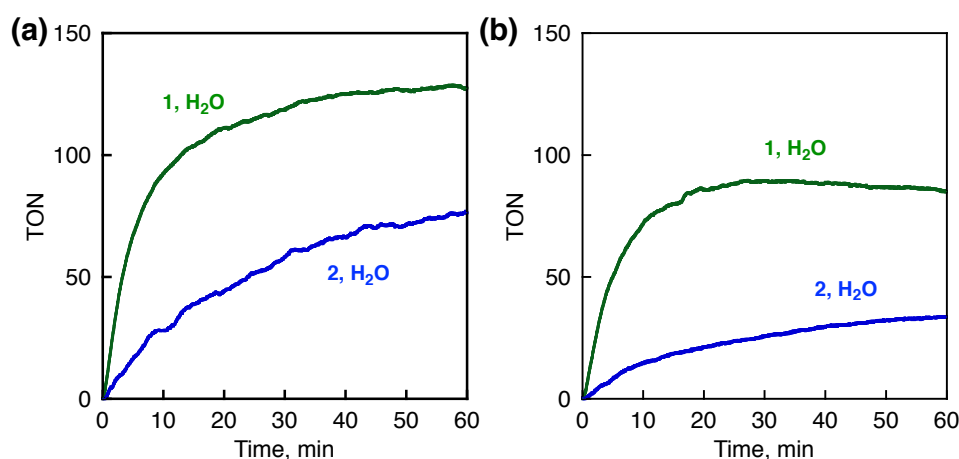


Figure S2. Time courses of O₂ evolution quantified by manometry in the catalytic water oxidation by CAN (125 mM) with **1** and **2** (12.5 μ M) in a non-buffered aqueous solution (2.0 mL). (a) Addition of CAN into iron complexes; CAN (250 μ mol) was dissolved in 0.20 mL water and added into 1.8 mL of iron complex solution (b) Addition of iron complexes into CAN; CAN (250 μ mol) was dissolved in 1.95 mL water in the reaction vial. The reaction was started by adding 50 μ L of iron complex solution into CAN solution.

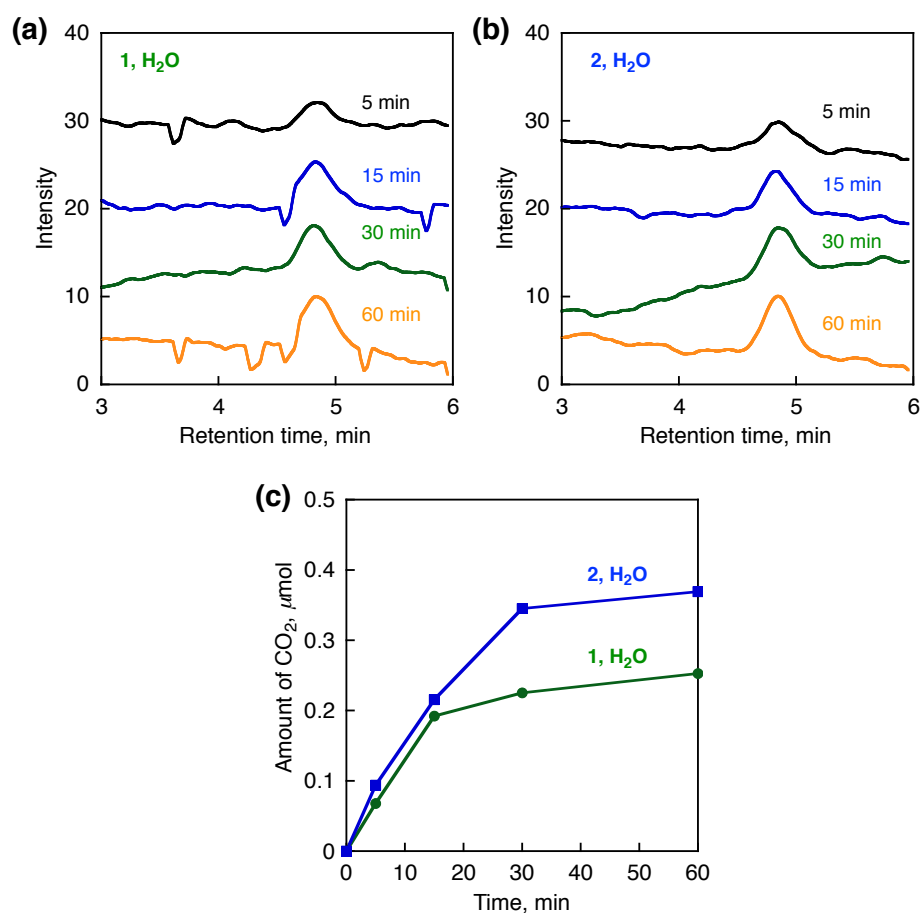


Figure S3. GC charts of CO₂ evolution in the catalytic water oxidation with (a) **1** (12.5 μM) and (b) **2** (12.5 μM) by CAN (125 mM) in a non-buffered aqueous solution (2.0 mL). (c) Time courses of CO₂ evolution with **1** (green circles) and **2** (blue squares) in the reaction.

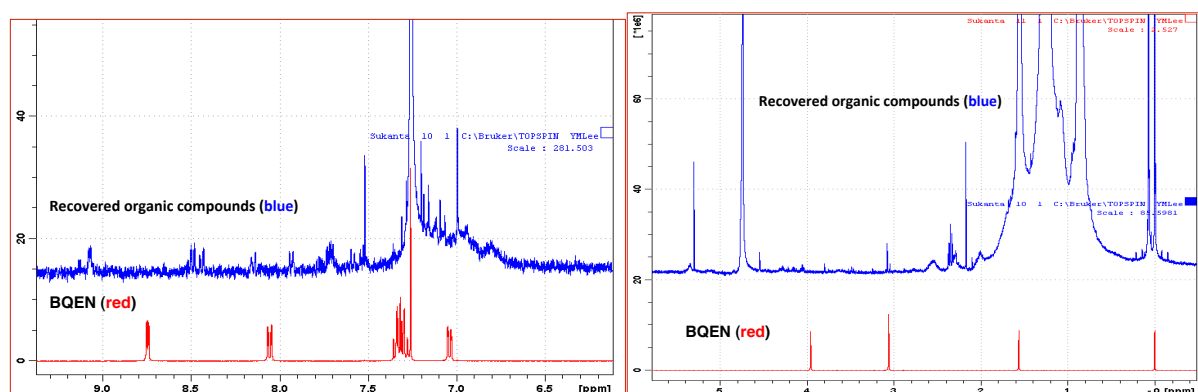


Figure S4. ^1H NMR spectra (in CDCl_3) of BQEN ligand (red line) and the organic material (blue line) obtained from the water oxidation reaction by CAN (0.10 M) with **1** (1.0 mM) in a non-buffered aqueous solution after 1 h. The organic compounds were collected as follows: H_2SO_4 was added to the resulting solution to remove the precipitates (cerium sulphate) formed in the solution by centrifugation, and a yellow-brown solution was obtained. Addition of excess KCN into the yellow-brown solution (to remove iron ions) generated brown precipitates along with a red solution. The precipitates were separated from the red solution by centrifugation. The precipitates and the red solution were washed separately with CH_2Cl_2 . Then the combined CH_2Cl_2 solutions were washed with water and dried over Na_2SO_4 . Finally, the yellow oily residue was obtained by removal of CH_2Cl_2 .

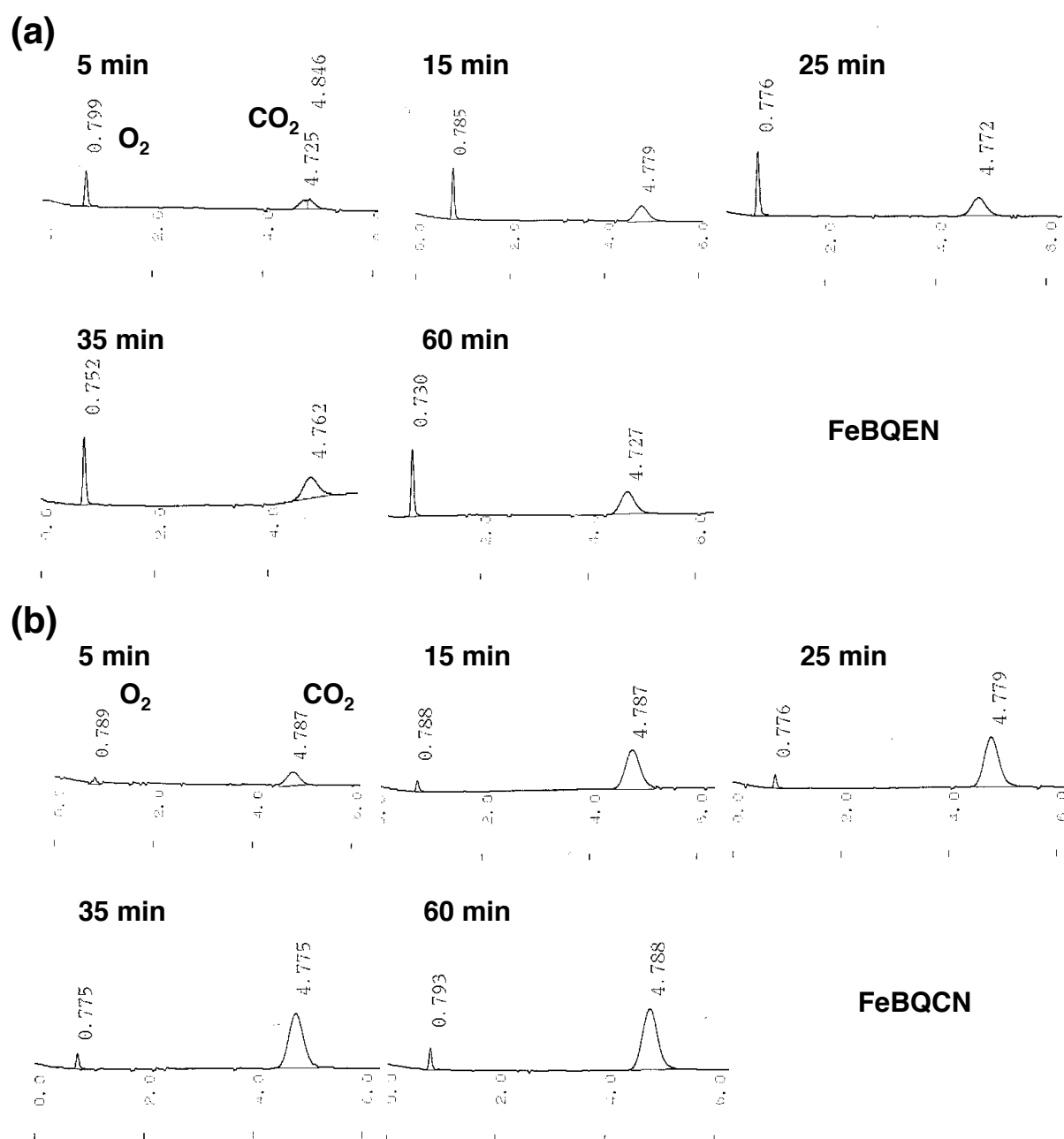


Figure S5. GC charts of CO_2 evolution observed with (a) **1** (1.0 mM) and (b) **2** (1.0 mM) in the catalytic reactions by CAN (0.10 M) in a non-buffered aqueous solution (2.0 mL).

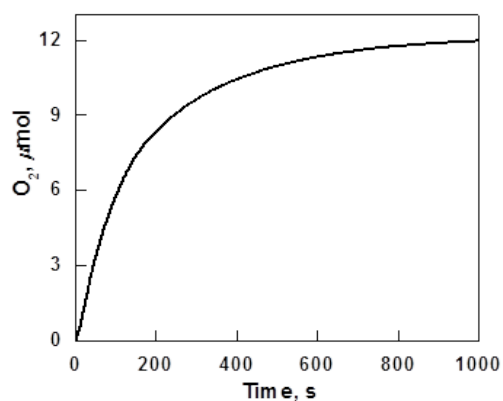


Figure S6. Time courses of O₂ evolution monitored by manometry in the catalytic water oxidation by CAN (0.10 M) with **1** (1.0 mM) in a non-buffered aqueous solution (2.0 mL).

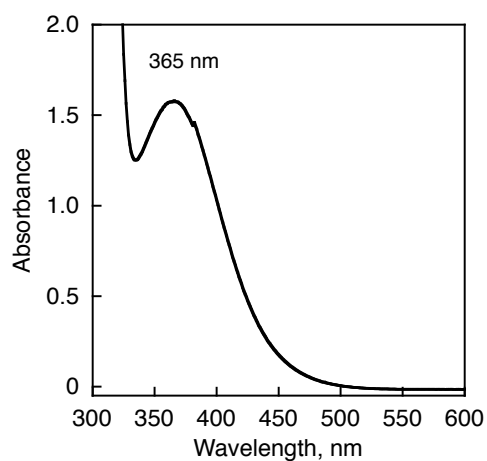


Figure S7. UV-vis spectra of an aqueous solution (2.0 mL) containing BQEN (1.0 mM) and HNO₃ (0.10 M).

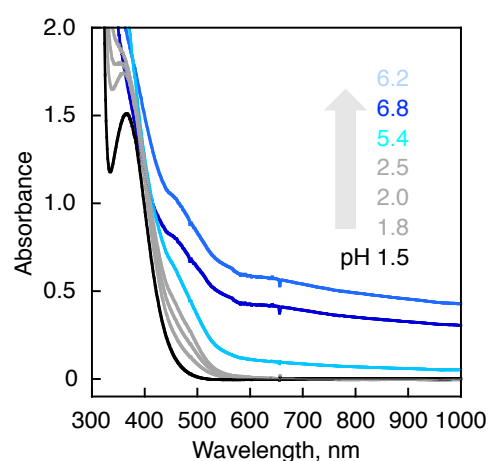


Figure S8. UV-vis spectral changes observed for the titration of an aqueous solution (2.0 mL) of **1** (1.0 mM) in HNO₃ (0.10 M) with NaOH.

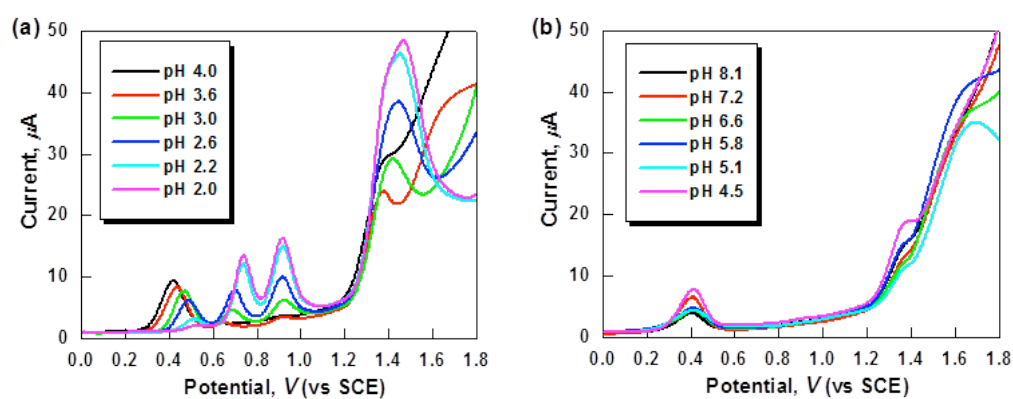


Figure S9. Differential pulse voltammetry (DPV) of an aqueous solution containing **1** (0.50 mM) and NaNO₃ (0.10 M) in different pH ranges: (a) from 2.0 to 4.0 and (b) from 4.5 to 8.1 (conditions: amplitude = 50 mV; pulse period = 0.2 s).

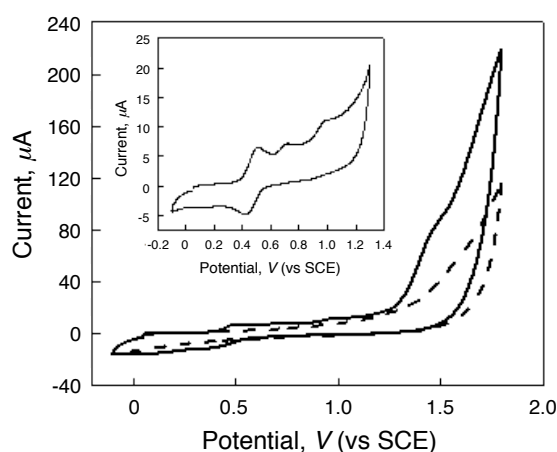


Figure S10. CVs of glassy carbon background (black dashed) and complex **1** (0.50 mM, black solid) in an aqueous solution (pH 3.4, 0.10 M NaNO₃) with scan rate of 100 mV s⁻¹. Inset shows the CV of **1** up to potential 1.3 V with a reversible Fe^{III/II} couple at $E_{1/2} = 0.47$ V followed by two dissociated BQEN ligand centered irreversible oxidation waves.

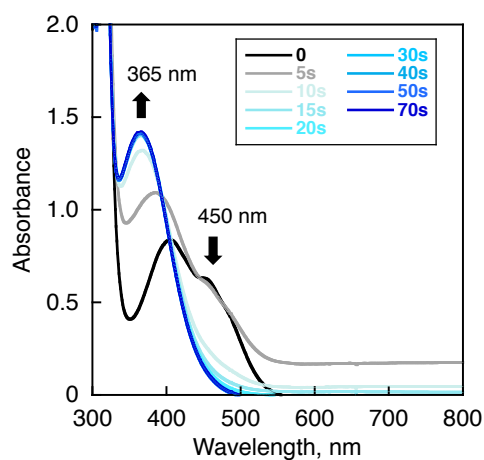


Figure S11. UV-vis spectral changes observed by adding HNO₃ (70 wt%, 20 μL) to **1** (1.0 mM) in a non-buffered aqueous solution (2.0 mL).

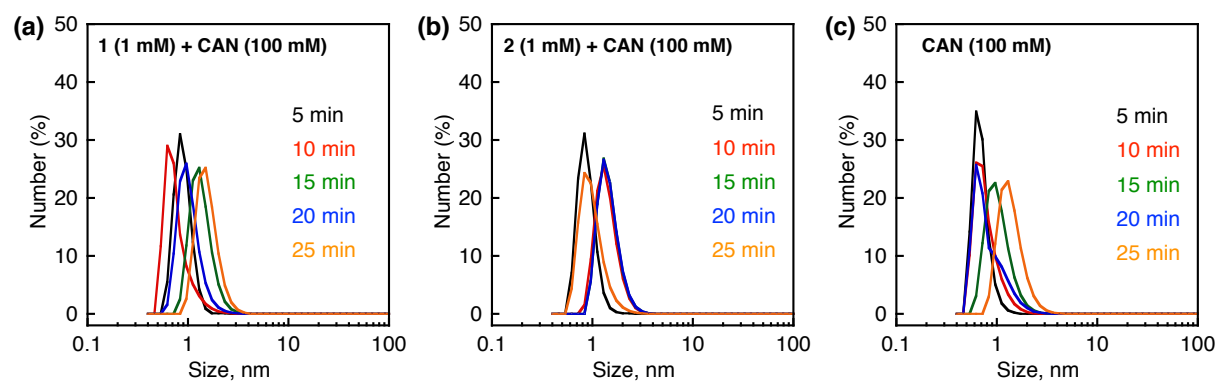


Figure S12. Particle size distribution determined by dynamic light scattering (DLS) measurements of non-buffered aqueous solutions of (a) **1** (1.0 mM) plus CAN (0.10 M), (b) **2** (1.0 mM) plus CAN (0.10 M), and (c) only CAN (0.10 M) at reaction times of 5.0 min (black line), 10 min (red line), 15 min (green line), 20 min (blue line), and 25 min (orange line).

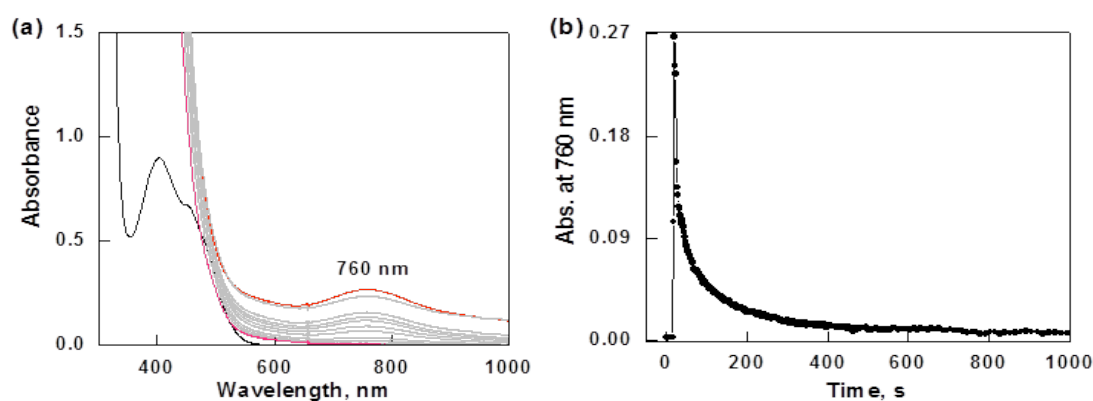


Figure S13. (a) UV-vis spectral changes observed in the water oxidation by CAN (0.10 M) in the presence of **1** (1.0 mM) in a non-buffered aqueous solution. (b) Time courses of the decay of absorption band at 760 nm due to $[\text{Fe}^{\text{IV}}(\text{BQEN})(\text{O})]^{2+}$ in the water oxidation by CAN (0.10 M) in the presence of **1** (1.0 mM).

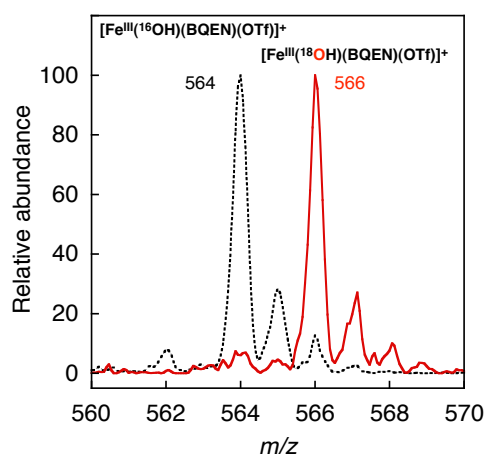


Figure S14. ESI-MS spectra of the solutions obtained in the reaction of **1** (1.0 mM) with CAN (2.0 mM) in H₂¹⁶O/MeCN [1:4 (v/v), black dots] and H₂¹⁸O/MeCN [1:4 (v/v), red line]. The peaks at *m/z* 564.0 and 566.0 correspond to [Fe^{III}(BQEN)(¹⁶OH)(OTf)]⁺ and [Fe^{III}(BQEN)(¹⁸OH)(OTf)]⁺ (calcd *m/z* = 564.1 and 566.1, respectively).

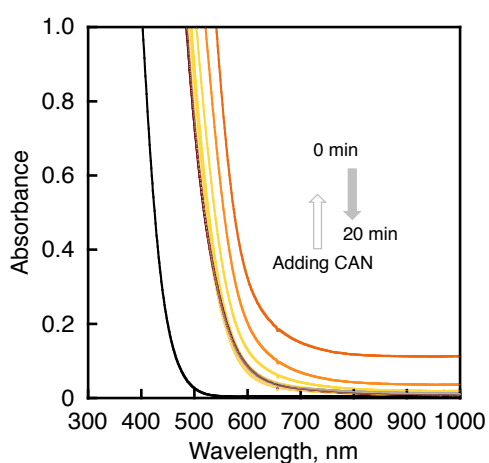


Figure S15. UV-vis spectral changes of an aqueous solution containing CAN (0.10 M), **1** (1.0 mM) and HNO₃ (0.10 M).

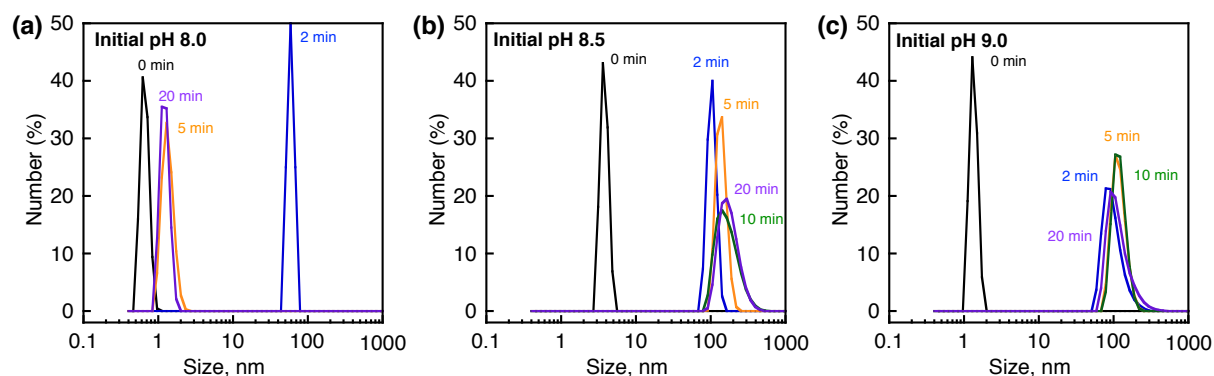


Figure S16. Particle size distribution determined by DLS measurements at initial pH (a) 8.0, (b) 8.5, and (c) 9.0 in borate buffer solutions containing **1** (5.0 μ M), $\text{Na}_2\text{S}_2\text{O}_8$ (5.0 mM) and $[\text{Ru}(\text{bpy})_3]\text{SO}_4$ (0.25mM) at the irradiation times of 2.0 min (blue line), 5.0 min (orange line), 10 min (green line), and 20 min (purple line). The black line shows the particle size distribution in the absence of **1** at 0 min.

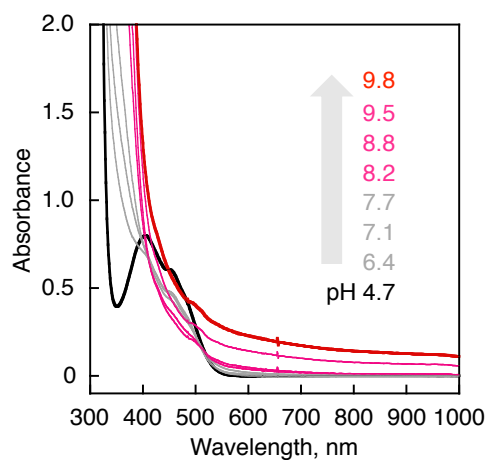


Figure S17. UV-vis spectral changes observed for the titration of a non-buffered aqueous solution (2.0 mL) containing **1** (1.0 mM) with NaOH.

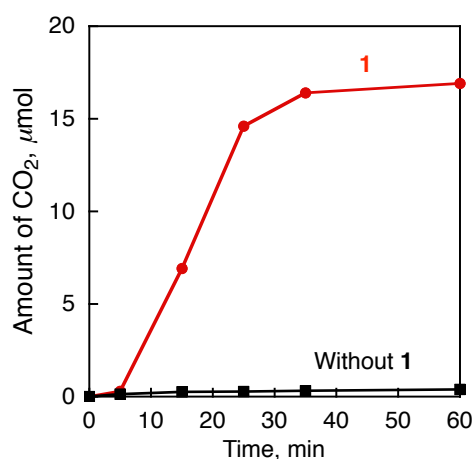


Figure S18. Time courses of CO₂ evolution under photoirradiation ($\lambda > 420$ nm) of a borate buffer solution (0.10 M, 2.0 mL) containing Na₂S₂O₈ (25 mM) and [Ru(bpy)₃]₂SO₄ (0.25 mM) in the absence (black squares) and presence of **1** (1.0 mM, red cycles). The CO₂ evolution was quantified by GC.

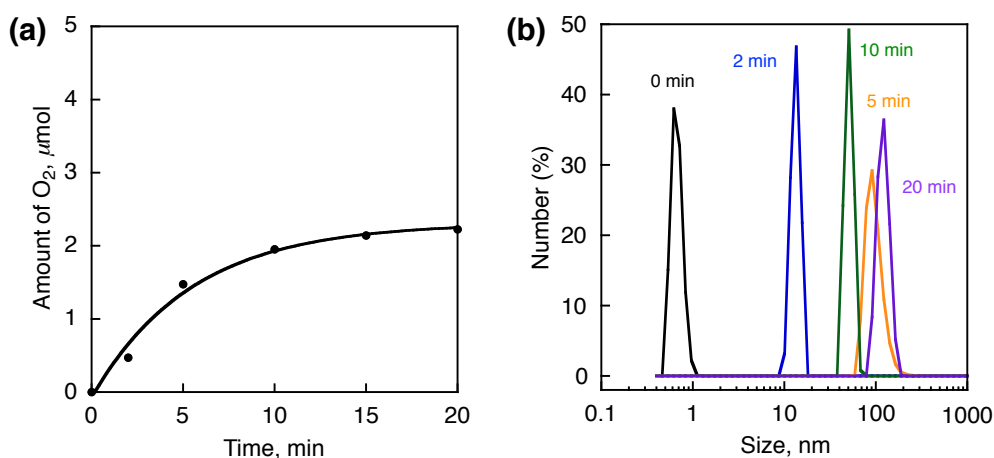


Figure S19. (a) Time course of O₂ evolution under photoirradiation ($\lambda > 420$ nm) of a borate buffer solution (0.10 M, 2.0 mL, initial pH 9.0) containing Na₂S₂O₈ (5.0 mM), [Ru(bpy)₃]₂SO₄ (0.25 mM), and **2** (5.0 μ M). (b) Particle size distribution determined by DLS measurements at initial pH 9.0 in a borate buffer solution containing **2** (5.0 μ M), Na₂S₂O₈ (5.0 mM) and [Ru(bpy)₃]₂SO₄ (0.25 mM) at the irradiation times of 2.0 min (blue line), 5.0 min (orange line), 10 min (green line), and 20 min (purple line). The black line shows the particle size distribution in the absence of **2** at 0 min.

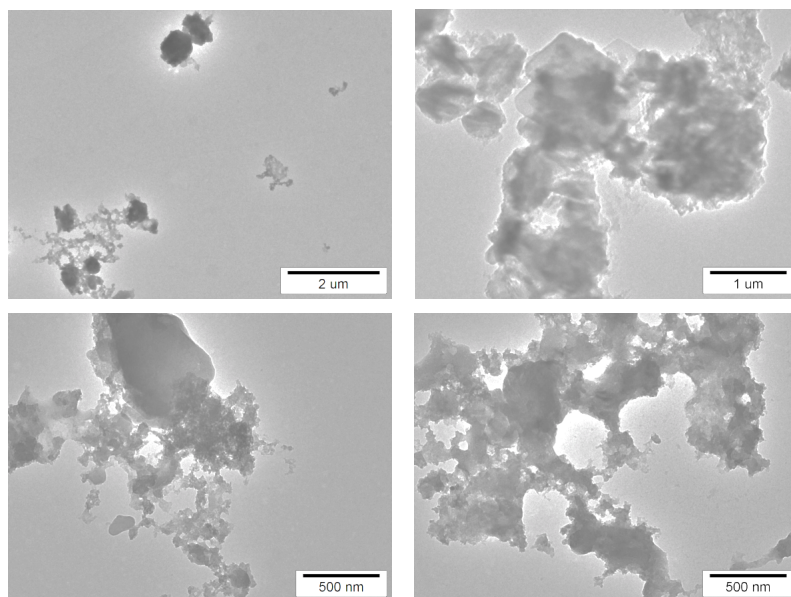


Figure S20. TEM images of the isolated particles formed in a borate buffer solution (0.10 M, 2.0 mL) containing $\text{Na}_2\text{S}_2\text{O}_8$ (5.0 mM), $[\text{Ru}(\text{bpy})_3]\text{SO}_4$ (0.25 mM) and **1** (1.0 mM).
